

# LINGO-1 Regulates Oligodendrocyte Differentiation through the Cytoplasmic Gelsolin Signaling Pathway

Zhaohui Shao, Xinhua Lee, Guanrong Huang, Guoqing Sheng, Christopher E. Henderson,  Daniel Louvard, Jiho Sohn, Blake Pepinsky, and  Sha Mi

Biogen, Inc., Cambridge, Massachusetts 02142

Differentiation and maturation of oligodendrocyte progenitor cells (OPCs) involve the assembly and disassembly of actin microfilaments. However, how actin dynamics are regulated during this process remains poorly understood. Leucine-rich repeat and Ig-like domain-containing Nogo receptor interacting protein 1 (LINGO-1) is a negative regulator of OPC differentiation. We discovered that anti-LINGO-1 antibody-promoted OPC differentiation was accompanied by upregulation of cytoplasmic gelsolin (cGSN), an abundant actin-severing protein involved in the depolymerization of actin filaments. Treating rat OPCs with cGSN siRNA reduced OPC differentiation, whereas overexpression of cGSN promoted OPC differentiation *in vitro* and remyelination *in vivo*. Furthermore, coexpression of cGSN and LINGO-1 blocked the inhibitory effect of LINGO-1. Our study demonstrates that cGSN works downstream of LINGO-1 signaling pathway, which enhances actin dynamics and is essential for OPC morphogenesis and differentiation. This finding may lead to novel therapeutic approaches for the treatment of demyelinating diseases such as multiple sclerosis (MS).

**Key words:** cytoplasmic gelsolin; LINGO-1; multiple sclerosis; oligodendrocyte; remyelination; therapeutic

## Significance Statement

Myelin loss and subsequent axon degeneration contributes to a variety of neurological diseases, such as multiple sclerosis (MS). Understanding the regulation of myelination by oligodendrocytes is therefore critical for developing therapies for the treatment of MS. We previously demonstrated that leucine-rich repeat and Ig-like domain-containing Nogo receptor interacting protein 1 (LINGO-1) is a negative regulator of oligodendrocyte differentiation and that anti-LINGO-1 promotes remyelination in preclinical animal models for MS and in a phase II acute optic neuritis clinical trial (RENEW). The mechanism by which LINGO-1 regulates oligodendrocyte differentiation is unknown. Here, we demonstrate that LINGO-1 regulates oligodendrocyte differentiation and maturation through the cytoplasmic gelsolin signaling pathway, providing new drug targets for the treatment of demyelination diseases.

## Introduction

Oligodendrocyte differentiation and myelination are tightly regulated processes that are essential to normal CNS development and function. Understanding how the processes are regulated should provide insights for developing new therapies for the treatment of demyelinating diseases such as multiple sclerosis

(MS). Many factors have been implicated in regulating oligodendrocyte progenitor cell (OPC) differentiation and maturation (Bercury and Macklin, 2015). OPC differentiation requires dynamic assembly and disassembly of actin microfilaments to allow the plasma membrane extension necessary for lamellipodia/filopodia growth, membrane protrusion, and focal adhesions (Bercury and Macklin, 2015). Two recent studies suggest that actin dynamics are regulated in distinct manners for different phases of myelination: actin assembly is required for oligodendrocyte process extension, whereas actin disassembly leads to myelin wrapping (Nawaz et al., 2015; Zuchero et al., 2015).

Actin exists in cells in filamentous (F-actin) and globular/monomeric (G-actin) states. The ratio of F-actin to G-actin, which is tightly controlled by actin-binding proteins such as gelsolin (dos Remedios et al., 2003), regulates cell morphology and can change rapidly under physiological conditions. Gelsolin is an abundant actin-binding protein and plays a critical role in the regulation of actin dynamics (Li et al., 2012). Gelsolin exists

Received Dec. 4, 2016; revised Jan. 19, 2017; accepted Feb. 6, 2017.

Author contributions: D.L. and S.M. designed research; Z.S., X.L., G.H., G.S., and J.S. performed research; G.H., C.E.H., B.P., and S.M. analyzed data; Z.S. and S.M. wrote the paper.

We thank Colin Smith and Chris-Ann McKenzie at University of Edinburgh for providing the fresh-frozen brain samples from human MS and non-MS patients for Western blot analysis, and Yun Bian for helping to harvest tissues from the animals.

The authors hold stock in Biogen, Inc.

D. Louvard's present address: Unité Mixte de Recherche 144 Centre National de la Recherche Scientifique/Institut Curie, Paris, France.

Correspondence should be addressed to Sha Mi, Ph.D., Department of Neurology Research, Biogen, Inc., 115 Broadway, Cambridge, MA 02142. E-mail: sha.mi@biogen.com.

DOI:10.1523/JNEUROSCI.3722-16.2017

Copyright © 2017 the authors 0270-6474/17/373127-11\$15.00/0

**Table 1.** Human MS brain tissues and sex- and age-matched control samples

| Group 1 (MS) |     |     |        | Group 2 (control) |     |     |  |
|--------------|-----|-----|--------|-------------------|-----|-----|--|
| #            | Sex | Age | Lesion | #                 | Sex | Age | Neuropath classifications  |
| 1            | F   | 42  | CL     | 21                | F   | 42  | No significant abnormalities   |
| 2            | F   | 53  | AL     | 22                | F   | 53  | No significant abnormalities   |
| 3            | F   | 53  | CL     | 23                | F   | 47  | No significant abnormalities   |
| 4            | F   | 44  | CL     | 24                | F   | 44  | No significant abnormalities   |
| 5            | M   | 46  | CAL    | 25                | M   | 46  | Control, vascular disease, other   |
| 6            | F   | 53  | AL/CAL | 26                | F   | 51  | No significant abnormalities   |
| 7            | M   | 45  | CL     | 27                | M   | 45  | No significant abnormalities   |
| 8            | F   | 57  | CL     | 28                | F   | 57  | Depression, recurrent; dependence, alcohol; control, vascular disease, other         |
| 9            | M   | 43  | CAL    | 29                | M   | 43  | No significant abnormalities   |
| 10           | F   | 48  | CAL    | 30                | F   | 48  | No significant abnormalities   |
| 11           | M   | 45  | AL     | 31                | M   | 44  | No significant abnormalities   |
| 12           | F   | 71  | CAL    | 32                | F   | 71  | Control, vascular disease, other   |
| 13           | F   | 71  | AL/CAL | 33                | F   | 71  | No significant abnormalities   |
| 14           | F   | 53  | CAL    | 34                | F   | 49  | No significant abnormalities   |
| 15           | F   | 42  | AL     | 35                | F   | 41  | No significant abnormalities   |
| 16           | F   | 50  | AL/CAL | 36                | F   | 50  | Control, vascular disease, other   |
| 17           | F   | 44  | AL     | 37                | F   | 44  | No significant abnormalities   |
| 18           | F   | 50  | CAL    | 38                | F   | 51  | No significant abnormalities   |
| 19           | F   | 48  | AL/CAL | 39                | F   | 49  | Control, substance abuse, alcohol; dependence, alcohol; no significant abnormalities |
| 20           | F   | 57  | AL     | 40                | F   | 57  | No significant abnormalities   |

AL, Active lesion; CAL, chronic active lesion; CL, chronic lesion.

in the extracellular (secreted, pGSN) and intracellular (cytoplasmic, cGSN) forms, which are expressed from an alternatively spliced gene under different promoters. pGSN contains an additional N-terminal 24 aa compared with cGSN (Kwiatkowski et al., 1986). Both forms of gelsolin are potent actin filament-severing proteins, converting F-actin to G-actin. pGSN plays an important role in the clearance of actin aggregates in the blood after tissue-injury-induced cell death (Lee and Galbraith, 1992; Spinardi and Witke, 2007; Bucki et al., 2008; Li-ChunHsieh et al., 2015). cGSN is ubiquitously expressed inside cells including myelin-forming oligodendrocytes. However, its function in OPC differentiation and myelination is unknown.

LINGO-1, a membrane protein selectively expressed in the CNS, has been identified as a negative regulator of oligodendrocyte differentiation and myelination (Mi et al., 2005; Mi et al., 2013). Blocking LINGO-1 function by antagonists including anti-LINGO-1 antibodies promotes oligodendrocyte differentiation and myelination *in vitro* and *in vivo* (Mi et al., 2007; Mi et al., 2009). Opicinumab (BIIB033), an anti-LINGO-1 antibody, improved visual evoked potentials in a phase II acute optic neuritis trial, suggesting a positive effect on remyelination (Cadavid et al., 2015). The downstream players that participate in the LINGO-1 signaling pathway remain unclear. Here, we report that cGSN plays a key role in oligodendrocyte differentiation, acting downstream of the LINGO-1 signaling pathway.

## Materials and Methods

**Quantitative RT-PCR.** RNA was isolated from cells using the Absolutely RNA Miniprep Kit (Agilent Technologies). Quantitative RT-PCR was used to quantify GSN and myelin basic protein (MBP) mRNA levels with  $\beta$ -actin used as an internal control. All primer sets were from Life Technologies, including custom-made cGSN and pGSN probes.

**Human brain samples.** Twenty fresh-frozen brain samples from 11 postmortem human secondary progressive MS patients and 20 age- and sex-matched samples from patients with no neuropathological abnormalities were provided by University of Edinburgh (approved by East of Scotland Research Ethics Service). Tissue attributes were characterized by immunohistochemistry staining performed by University of Edinburgh (for details, see Table 1). Each sample was lysed with RIPA buffer (50 mM Tris, pH 7.2, 1% Triton X-100, 0.5% sodium deoxycholate, 0.1% SDS, 150 mM NaCl, 10 mM MgCl<sub>2</sub>, 5% glycerol) at 1 ml per 0.2 mg of

tissue. Equal amounts of protein were loaded onto 4–15% SDS-PAGE gel and subjected to Western blot analysis probed with antibodies against LINGO-1 (3C11, 2  $\mu$ g/ml; Biogen), GSN (12953, RRID: AB-2632961, 1:1000; Cell Signaling Technology), or pGSN (NBP2-27566, RRID: AB-2632960, 2  $\mu$ g/ml; Novus Biologicals). Western blot membranes were then stripped and reprobed with anti-GAPDH (NB600-502, RRID: AB-350715, 1:5000 or NB100-56875, RRID: AB-838305, 1:500; Novus Biologicals) as loading controls. Band intensities of the Western blot TIFF images were quantified by the Image Studio software (LI-COR).

**Primary OPC culture.** Enriched populations of rat OPCs were purified as described previously (Mi et al., 2005) and maintained in a defined DMEM (DMEM with 4 mM glutamine, 1 mM sodium pyruvate, 0.1% w/v bovine serum albumin, 50  $\mu$ g/ml apo-transferrin, 5  $\mu$ g/ml insulin, 30 nM sodium selenite, 10 nM D-biotin, and 10 nM hydrocortisone) plus 10 ng/ml FGF and PDGF (Peprotech). For differentiation, the A2B5<sup>+</sup> OPCs were cultured on PDL-coated plates (Fisher) in the defined DMEM supplemented with 15 nM T3 (Sigma-Aldrich) and 10 ng/ml ciliary neurotrophic factor (Peprotech) for 3 d with 2  $\mu$ g/ml anti-LINGO-1 antibody (BIIB033; Biogen) or an aglycosyl IgG1 isotype control antibody (5C8; Biogen). All experiments related to OPC differentiation were repeated two to three times with two biological replicates for each experiment.

For transfection of plasmid or siRNA into OPCs, the electroporation method was used with an Amaxa kit (Lonza). Transfected OPCs were then plated onto PDL-coated plates in growth medium and then switched to differentiation medium for 3 d as described above. All siRNAs were from Life Technologies, including custom-ordered cGSN and pGSN-specific siRNA. Rat GSN siRNA (ID# s150340), sense sequence (5'–3') GGACAGUUUC AACACGGUtt. Rat cGSN siRNA (ID# s529615), sense sequence (5'–3') CCACAGCAGGUACCAAtt. Rat pGSN siRNA (ID# s529575), sense sequence (5'–3') CAAAGUCGGGUGUCUGAGAtt.

For assessing protein expression by Western blot, cells were lysed in RIPA buffer and Western blots were performed as described above using antibodies to MBP (SMI-94 and SMI-99, RRID: AB-87330 and AB-2314772, 1:4000 mixture of each; BioLegend), MAG (34-6200, RRID: AB-87330, 1:1000; Life Technologies), myelin oligodendrocyte glycoprotein (MOG; MAB5680, RRID: AB-1587278, 1:10,000; Millipore), CNPase (ab6319, RRID: AB-2082593, 2  $\mu$ g/ml; Abcam), GSN (12953S, RRID: AB-2632961, 1:1000; Cell Signaling Technology), phosphorylated-cofilin-1 (C8992, RRID: AB-1078547, 1:2000; Sigma-Aldrich), cofilin-1 (ab42824, RRID: AB-879739, 1:5000; Abcam), CAP-1 (ab155079, RRID: AB-2632962, 1:1000; Abcam), ArpC3 (612234, RRID: AB-399557, 1:1000; BD Biosciences), GAPDH

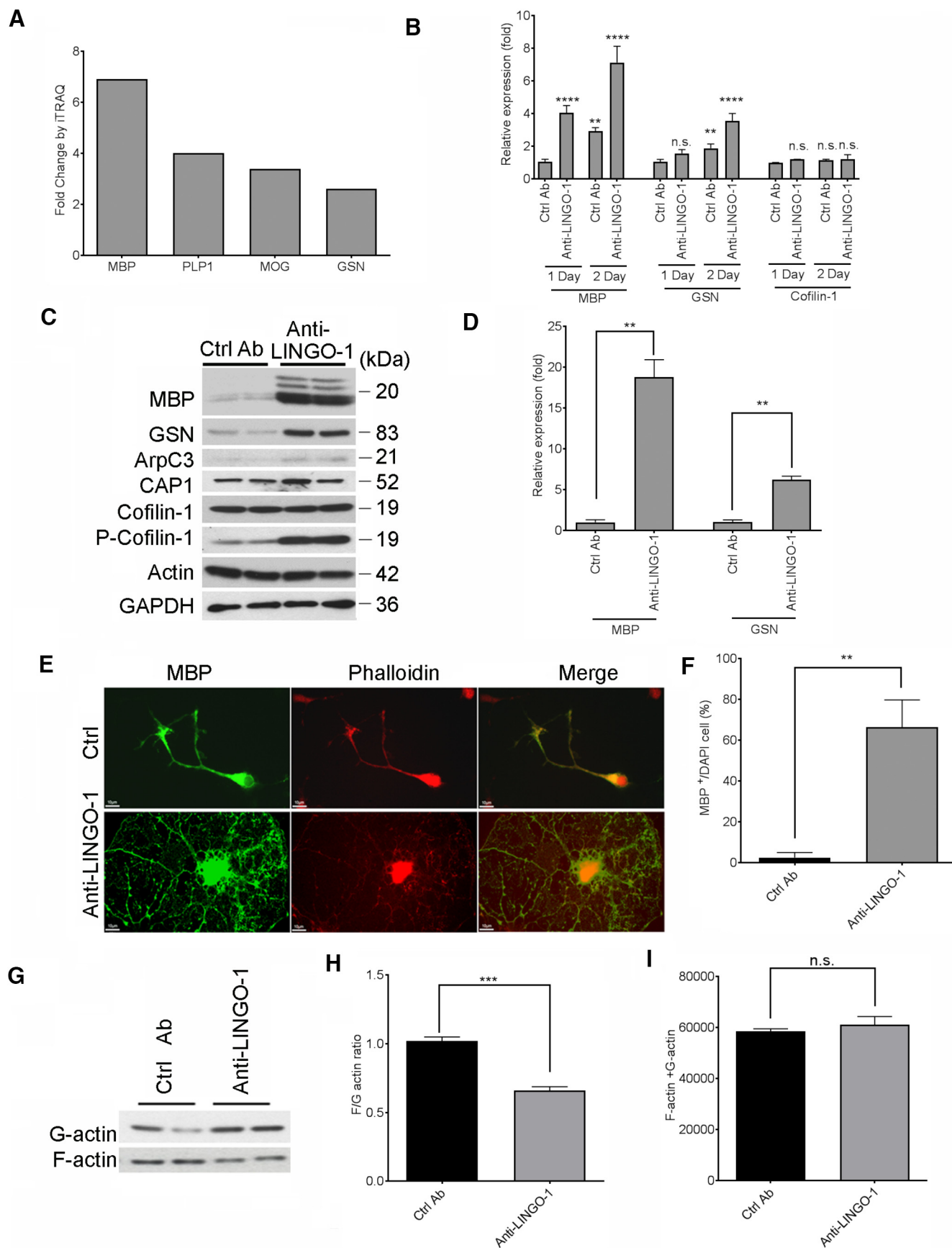


**Figure 1.** Increased gelsolin expression and actin disassembly after anti-LINGO-1 antibody-induced oligodendrocyte differentiation. **A**, Proteins showing increased expression in oligodendrocytes after 3 d treatment of the anti-LINGO-1 antibody versus levels after control antibody treatment, quantified by iTRAQ proteomic analysis. **B**, Quantitative PCR analysis of MBP, GSN, and Cofilin-1 mRNA expression levels in primary rat OPCs cultured in differentiation medium treated with anti-LINGO-1 or control antibody (Ctrl Ab) for 1 or 2 d, with (Figure legend continues.)

(NB600-502, RRID: AB-350715, 1:5000; Novus Biologicals), and actin (4968S, RRID: AB-10695740, 1:1000; Cell Signaling Technology).

The G-actin/F-actin *in vivo* assay kit (BK037; Cytoskeleton) was used for the biochemical quantification of F-actin and G-actin amounts in OPCs. Briefly, cells were lysed in LAS2 buffer at 37°C for 10 min. After a 5 min room temperature centrifugation step at  $350 \times g$  to remove cell debris, the lysate were subjected to ultracentrifuge at  $100,000 \times g$  for 1 h at 37°C. The supernatant containing G-actin was removed and the pellet containing F-actin was solubilized to the equal volume with F-actin depolymerization buffer. Initial volumes of G-actin and F-actin fractions were analyzed by Western blot for actin. All reagents used in the assay were supplied by the kit. Band intensities of the Western blot TIFF images were quantified with Image Studio software (LI-COR).

**Immunofluorescence.** All procedures were performed at room temperature. Cells cultured on chamber slides were fixed in 4% paraformaldehyde for 30 min, blocked, and permeabilized in 10% normal goat serum and 0.1% Triton X-100 in PBS. MBP stainings were done by incubation with anti-MBP antibody (SMI-94 and SMI-99, RRID: AB-87330 and AB-2314772, 1:500; BioLegend) in blocking buffer for 2 h, followed by Alexa Fluor 488-labeled goat anti-mouse IgG (A11029, RRID: AB-2534088, 1:500; Life Technologies) in blocking buffer for 1 h. For F-actin staining, cells were incubated with Alexa Fluor 594-phalloidin (A12381, RRID: AB-2315633, 5 units/ml; Life Technologies) at room temperature for 1 h. Slides were mounted with Prolong Gold mounting media containing DAPI (P36931; Life Technologies). Images were taken using a Leica DMR epifluorescence microscope with  $63\times$  oil lens or Olympus VS120 slide scanner with  $20\times$  lens. Image quantification was done with Visiopharm software. For MBP quantification, MBP<sup>+</sup> cells per image were counted or quantified by the total area of MBP<sup>+</sup> fluorescent signal divided by the number of DAPI<sup>+</sup> cells.

**Proteomic analysis.** Primary rat OPCs cultured in differentiation medium in the presence/absence of 2  $\mu\text{g/ml}$  anti-LINGO-1 antibody (BIIB033; Biogen) for 3 d were lysed in digestion buffer (50 mM HEPES, 150 mM NaCl, 1 mM EDTA, 4% Rapigest) by sonication. Cell lysates were centrifuged and supernatants were reduced, alkylated, and trypsin digested overnight as described previously (Ross et al., 2004). The resulting peptide mixtures were iTRAQ labeled and subsequently combined into six four-plex mixtures. Each of these four-plex mixtures was analyzed by 2D nanoliquid chromatography mass spectrometry with strong cation exchange and reverse phase as the first and second dimension, respectively.

**Animal care.** All animal handling and surgical procedures followed the protocols approved by the Biogen Institutional Animal Care and Use Committee.

**Mouse samples.** Heterozygous (Het) *Shiverer* mice were purchased from The Jackson Laboratory (<https://www.jax.org/strain/001428>) and bred in house as Het  $\times$  Het. Mice were housed in cages of two to five animals in 12/12 h light/dark cycles. Fresh-frozen brain and spinal cord samples from P30 homozygous *Shiverer* mice and wild-type littermates

(1 male and 1 female) were collected after perfusion with PBS, lysed in RIPA buffer and subjected to Western blot analysis as described above for human brain samples and primary OPC culture.

**Lyssolecithin (LPC)-induced demyelination rat model.** Nine-week old female Sprague Dawley rats (<http://www.criver.com/products-services/basic-research/find-a-model/sprague-dawley-rat>) were anesthetized by isoflurane inhalation. Body temperature was monitored and animals were kept on an electric heating pad during anesthesia. Aseptic technique was used throughout the procedure. AAV9 viruses ( $4.8 \times 10^{10}$  genome copy in 20  $\mu\text{l}$ ) encoding cGSN or GFP were intrathecally injected into cisterna magna 14 d before LPC injection. LPC (4  $\mu\text{l}$  of 1% in saline; L1381, Sigma-Aldrich) was injected into the dorsal column to induce demyelination in spinal cord. Animals were killed 9 d after LPC injection and the region of the spinal cord encompassing the lesion was excised and sectioned. Remyelinated axons in the lesions were quantified by toluidine blue staining of 1  $\mu\text{m}$  transverse thin sections. Representative images of remyelinated axons were taken by electron microscopy. Studies were performed double blinded. cDNA encoding rat cGSN with C-terminal Flag tag was cloned into an AAV vector under the CAG promoter provided by Vector Biolabs. The production and titering of the AAV9-CAG-GFP or AAV9-CAG-cGSN viruses were performed by Vector Biolabs. GSN protein expression from the AAV-GSN viruses was confirmed by Western blot of transduced 293 cells as described above.

**Statistics.** The data collection and analysis were performed blinded. GraphPad Prism 6 software was used for statistical analysis. Comparison of mean values was conducted with unpaired Student's *t* tests or one-way ANOVA. In all analyses, statistical significance was determined at the 5% level ( $p < 0.05$ ). No data were excluded from the analyses. Data are presented as mean  $\pm$  SD except for those shown in Figure 5B, which are shown as mean  $\pm$  SEM. No statistical methods were used to predetermine sample sizes, which were chosen based on previous literature in the field. Data distribution was assumed to be normal, but this was not formally tested.

**Data availability.** Original data are available from the corresponding author upon reasonable request.

## Results

### Gelsolin is upregulated in OPC differentiation

To unravel the molecular determinants of LINGO-1 function in oligodendrocyte biology, we performed a proteomic profiling study of primary rat OPCs. Anti-LINGO-1 antibody-induced oligodendrocyte differentiation was associated with increased protein expression of myelin components, such as MBP, proteolipid protein-1, and MOG. We discovered that GSN was also upregulated among the proteins most affected by anti-LINGO-1 treatment (Fig. 1A). We confirmed by quantitative PCR and Western blot analysis that anti-LINGO-1 antibody treatment increased GSN expression (Fig. 1B–D). When OPCs were cultured in differentiation medium without anti-LINGO-1, basal levels of GSN and MBP increased slightly as cells differentiated slowly over time. Anti-LINGO-1 antibody treatment accelerated the differentiation, as demonstrated by significant upregulation of MBP mRNA levels at 1 and 2 d. Notably, levels of GSN were also upregulated (Fig. 1B). By 3 d, MBP and GSN protein levels were increased 19- and 6-fold over control antibody-treated cells, respectively (Fig. 1C,D). Immunocytochemistry (ICC) of the cultures revealed a correspondingly significant increase in the percentage of differentiated oligodendrocytes (Fig. 1E,F). Despite the effect on GSN, anti-LINGO-1 treatment had little or no effect on Arp2/3 complex subunit 3 (ArpC3) or adenyl cyclase-associated protein (CAP-1), two ubiquitously expressed proteins that have been implicated in the control of actin dynamics. Interestingly, although the amount of cofilin-1 did not change (Fig. 1B,C), phosphorylated cofilin-1 increased approximately 4-fold upon anti-LINGO-1 treatment (Fig. 1C).

Because cGSN is an actin disassembly factor that functions through its capping and severing activities, we next determined

←

(Figure legend continued.) the expression in the sample treated by the Ctrl Ab for 1 d as 1. *p*-values were calculated by one-way ANOVA with Dunnett's multiple comparisons for each transcript, all compared with Ctrl Ab sample at 1 d (\*\* $p < 0.01$ , \*\*\*\* $p < 0.001$ , n.s., not significant). **C**, Western blot analysis of GSN and MBP from rat OPCs differentiated for 3 d in the presence/absence of anti-LINGO-1 antibody. **D**, Quantification of MBP and GSN as shown in **C** with Image Studio software (LI-COR) and represented as the band intensity relative to actin with the value of Ctrl Ab-treated sample was set as 1.  $p = 0.0073$  (MBP),  $p = 0.0051$  (GSN), by two-tailed unpaired Student's *t* test. **E**, ICC of rat OPCs differentiated for 3 d and immunostained for MBP (green) and phalloidin (red). Scale bar, 10  $\mu\text{m}$ . **F**, Quantification of MBP<sup>+</sup> cells as a percentage of total cells (DAPI<sup>+</sup>). Average 10 fields per slide, total 3 slides. ( $p = 0.0012$ , by two-tailed unpaired Student's *t* test.) **G**, Western blot analysis of F- and G-actin fractions from rat OPCs differentiated for 3 d in the presence/absence of anti-LINGO-1 antibody and separated according to the G-actin/F-actin *in vivo* assay kit (Cytoskeleton). **H**, Quantification of the band intensities of F- and G-actin shown in **G** and presented as F- to G-actin ratio.  $p = 0.0152$ ; two-tailed unpaired Student's *t* test. **I**, Quantification of total actin (F-actin + G-actin) level in **G**.  $n = 2$  experiments, with 2 biological replicates per experiment.  $p = 0.2243$ .



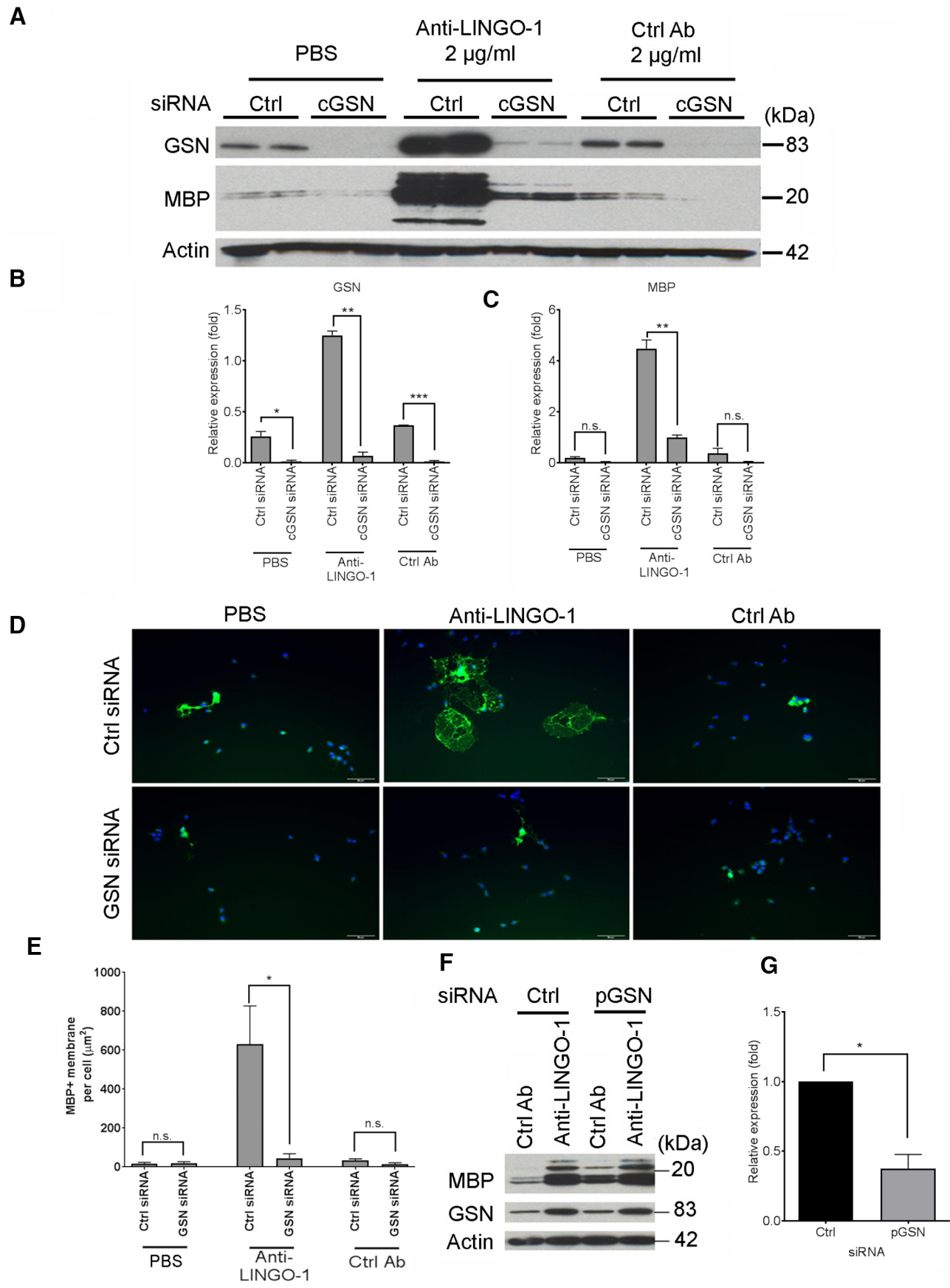


**Figure 2.** Anti-LINGO1 antibody-induced OPC differentiation is inhibited by GSN siRNA. **A**, Western blot analysis of MBP and GSN protein levels in rat primary OPCs transfected with Ctrl or cGSN siRNA and then differentiated for 3 d in the presence of the anti-LINGO-1 antibody or a Ctrl Ab. **B**, Quantification of the Western blot of GSN in **A** with Image Studio software (LI-COR) and represented as the band intensity relative to actin.  $p = 0.0192$  (PBS),  $p = 0.0011$  (anti-LINGO-1),  $p = 0.0004$  (Ctrl Ab) by two-tailed unpaired Student's *t* test. (Figure legend continues.)

whether anti-LINGO-1 treatment decreased F-actin microfilaments using fluorescent phalloidin staining (Zuchero et al., 2015). In control antibody-treated cultures, poorly differentiated oligodendrocytes with very few processes showed strong phalloidin labeling and poorly differentiated cell morphology. In contrast, anti-LINGO-1 antibody treatment led to strong MBP staining and poor phalloidin staining in processes (Fig. 1E). Levels of F- and G-actin in oligodendrocytes were further determined by biochemical separation and analyzed by Western blot. The F-actin/G-actin ratio in the cells treated with anti-LINGO-1 antibody was decreased by 40% versus control-treated cells, with no significant change in total actin (Fig. 1G–I). Therefore, OPC differentiation promoted by anti-LINGO-1 antibody correlates with a decrease in F-actin and an increase in G-actin levels, potentially reflecting the selective increase in GSN.

### cGSN is required for OPC differentiation

Actin dynamics, triggered by actin depolymerizing proteins such as GSN, is a necessary step to promote actin disassembly/reassembly into new structures such as lamellipodia and filopodia, the formation of which is required for OPC differentiation (Bauer et al., 2009). To explore the role of GSN and actin disassembly in OPC differentiation, siRNAs against either total GSN or cGSN were tested and gave similar results. cGSN siRNA treatment significantly reduced both the mRNA and protein levels of GSN in OPCs (Fig. 2A, B, and mRNA data not shown). Strikingly, cGSN siRNA treatment inhibited OPC differentiation induced by anti-LINGO-1 antibody, reducing MBP protein expression by 78% (Fig. 2A, C). We also observed strong inhibition of membrane process formation by cGSN siRNA (Fig. 2D, E). This study suggests that cGSN is required for OPC differentiation. In contrast, pGSN-specific siRNA had no effect on OPC differentiation in the presence of anti-LINGO-1 antibody treatment (Fig. 2F) despite decreasing corresponding pGSN mRNA levels by ~60% (Fig. 2G). Therefore, cGSN, but not pGSN, is required for OPC differentiation.

To further confirm the effect of cGSN on OPC differentiation, we overexpressed either cGSN or pGSN in OPCs by transfection. Overexpression of cGSN promoted cell differentiation. We observed a 10-fold increase in MBP protein production by Western blot and a 15-fold increase in the number of MBP<sup>+</sup> myelin sheet-forming cells by ICC (Fig. 3A–D). In contrast, overexpression of pGSN did not promote OPC differentiation (Fig. 3A–D). We further confirmed the pGSN overexpression result by treating OPCs with purified pGSN protein. Similar to the pGSN overexpression data, pGSN protein treatment did not increase MBP expression (Fig. 3E) compared with control antibody treatment. This result further suggests that cGSN, but not pGSN, is involved in promoting OPC differentiation.

Previous studies have shown that LINGO-1 inhibits OPC differentiation (Mi et al., 2005). To determine whether cGSN func-

tions downstream of the LINGO-1 OPC differentiation pathway, we looked at the effect of overexpressing cGSN and/or LINGO-1 on MBP expression. As shown in Figure 3F, overexpression of both LINGO-1 and cGSN at the same time induced MBP production to similar levels as seen in cells transfected with cGSN plasmid alone, indicating that overexpression of LINGO-1 did not block cGSN-induced OPC differentiation. In contrast, overexpression of both LINGO-1 and pGSN did not promote OPC differentiation. Together, our data showed that cGSN, but not pGSN, is required for OPC differentiation and that cGSN works downstream of LINGO-1.

### cGSN is downregulated in *Shiverer* mice spinal cord and brain and human MS brain tissues

To further explore the connection between cGSN and myelination, we measured GSN levels in spinal cord and brain lysates of *Shiverer* mice, which have hypomyelination in CNS due to the lack of MBP protein (Chernoff, 1981). As expected, MBP protein was not detectable in spinal cord and brain lysates of *Shiverer* mice (Fig. 4A). As reported previously, we also observed lower levels of MOG and MAG in *Shiverer* mice and that CNPase levels did not change (Mikoshihita et al., 1980). cGSN levels were 2- to 3-fold lower in *Shiverer* mice spinal cord and brain than in wild-type littermates (Fig. 4A, B), which is consistent with our finding that cGSN expression correlates with oligodendrocyte differentiation and maturation.

Because LINGO-1 and cGSN levels showed an inverse correlation during oligodendrocyte differentiation, we examined MS lesions, in which LINGO-1 is upregulated, to determine whether cGSN is downregulated. For this purpose, we examined the protein levels of LINGO-1 and GSN from 20 MS (5 chronic lesions, 5 active lesions, 6 chronic active lesions, and 4 active/chronic active lesions as listed in Table 1) and 20 sex- and age-matched non-MS brain tissues by Western blot analysis. Consistent with our finding, LINGO-1 levels increased by 4-fold and cGSN levels decreased by ~5-fold across all types of MS tissues compared with non-MS controls (Fig. 4C–F). pGSN levels in MS tissue were below the detection limit (data not shown).

### cGSN overexpression promotes remyelination *in vivo*

Because cGSN is required for OPC differentiation *in vitro*, we next tested whether cGSN overexpression promoted remyelination in the rat LPC model in which LPC was injected into the spinal cord to induce local demyelination (Fig. 5). AAV virus containing genes for cGSN or GFP as a control were administered to the animals 14 d before LPC injection. GSN expression in oligodendrocytes in LPC lesions was confirmed by immunohistochemistry (data not shown). Remyelination was evaluated by toluidine blue staining on 1  $\mu$ m thin sections 9 d after LPC injection (Fig. 5A). As shown in Figure 5, AAV-cGSN-treated rats contained ~1.7-fold more remyelinated axons than AAV-GFP-treated rats. This result is consistent with our *in vitro* data showing the critical role of cGSN in OPC differentiation and maturation.

## Discussion

MS is caused by inflammation and demyelination in the CNS. Demyelinated axons continue to degenerate and the accumulative axonal loss in chronic lesions leads to irreversible disability for the MS patients. Current treatments focus on managing the inflammation to slow the relapse rate. There is a large unmet need for therapies that can restore myelination and repair the damaged axons (Kremer et al., 2015; Najm et al., 2015; Kremer et al., 2016; Mei et al., 2016; Thiruvalluvan et al., 2016; Yao et al., 2016). The reasons for remyeli-

(Figure legend continued.) **C**, Quantification of the Western blot of MBP in **A** as done in **B**.  $p = 0.525$  (PBS);  $p = 0.0052$  (anti-LINGO-1);  $p = 0.1411$  (Ctrl Ab). **D**, OPCs transfected with Ctrl or GSN siRNA were immunostained for MBP (green). Blue, DAPI. Scale bar, 50  $\mu$ m. **E**, Quantification of myelin-like membrane area per cell shown in **D**. Average 4 fields per slide.  $n = 2$  biological replicates.  $p = 0.7023$  (PBS);  $p = 0.0247$  (anti-LINGO-1);  $p = 0.1349$  (Ctrl Ab); two-tailed unpaired Student's  $t$  test. **F**, Western blot analysis of MBP and GSN protein levels in primary OPCs transfected with Ctrl or pGSN-specific siRNA and then differentiated for 3 d. **G**, Quantification of pGSN mRNA expression level 48 h after siRNA transfection as in **F**. The expression in control siRNA-treated samples was set as 1.  $n = 2$  biological replicates.  $p = 0.0127$  by two-tailed unpaired Student's  $t$  test.

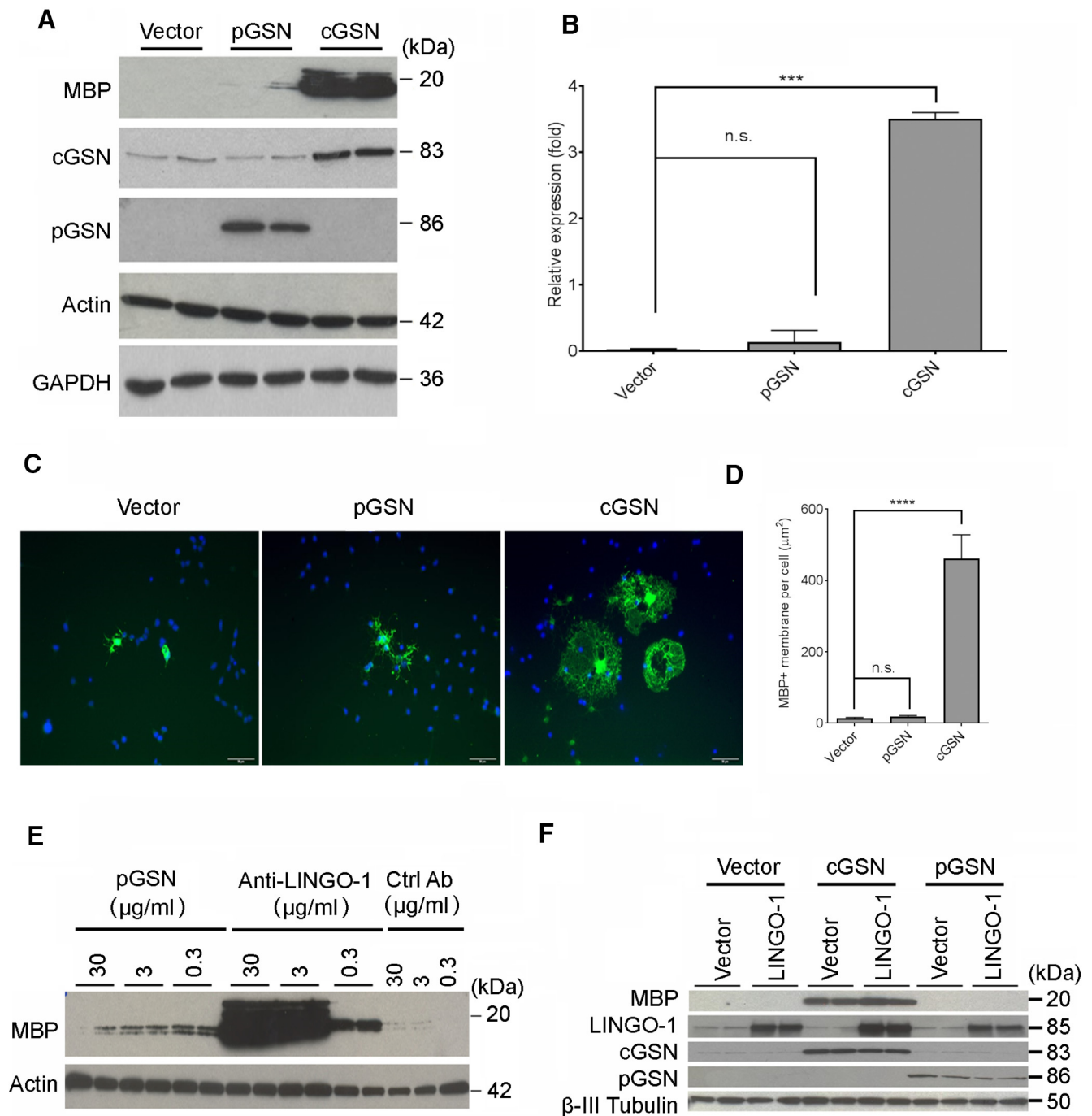


**Figure 3.** Overexpression cGSN promotes OPC differentiation. **A**, Western blot analysis of MBP, GSN, actin, and GAPDH protein expression in OPCs transfected with plasmids expressing cGSN, pGSN, or control vector for 3 d. pGSN expression was quantified in the culture medium. All other proteins were quantified from cell lysates. **B**, Quantification of the MBP protein shown in **A**, represented as band intensity relative to actin. *p*-values were calculated by one-way ANOVA with Dunnett's multiple comparisons compared with vector. \*\*\**p* < 0.005, n.s., not significant. **C**, OPCs treated as in **A** were immunostained by anti-MBP antibody (green). Blue, DAPI. Scale bar, 50 μm. **D**, Quantification of myelin-like membrane area per cell shown in **C**. Average 6 fields per slide. *n* = 2 biological replicates. *p*-values were calculated by one-way ANOVA with Dunnett's multiple comparisons compared with vector. n.s., not significant; \*\*\*\**p* < 0.001. **E**, Western blot analysis of MBP and actin expression in OPCs treated with recombinant pGSN or anti-LINGO-1 antibody for 3 d. **F**, Western blot analysis of MBP, GSN, LINGO-1, and β-III tubulin in OPCs transfected with plasmids expressing cGSN, pGSN, or control vector plus/minus a plasmid expressing LINGO-1 for 3 d.

nation failure in MS are poorly understood. The presence of significant numbers of OPCs within demyelinated lesions or plaques suggests that inhibitory mechanisms in the lesions block OPC differentiation and maturation, thereby preventing them from myelinating the damaged axons (Chang et al., 2000).

Oligodendrocyte differentiation from bipolar OPCs to mature oligodendrocytes involves dramatic morphological changes

that are regulated by actin microfilament dynamics (Bauer et al., 2009). These morphological changes are closely linked to the myelination process. Recent studies suggest that actin assembly is first required for initial outgrowth of actin-rich structures, lamellipodia, and filopodia and then actin disassembly is required for myelin sheet formation and myelination (Nawaz et al., 2015; Zuchero et al., 2015). Our data are in agreement that actin disas-

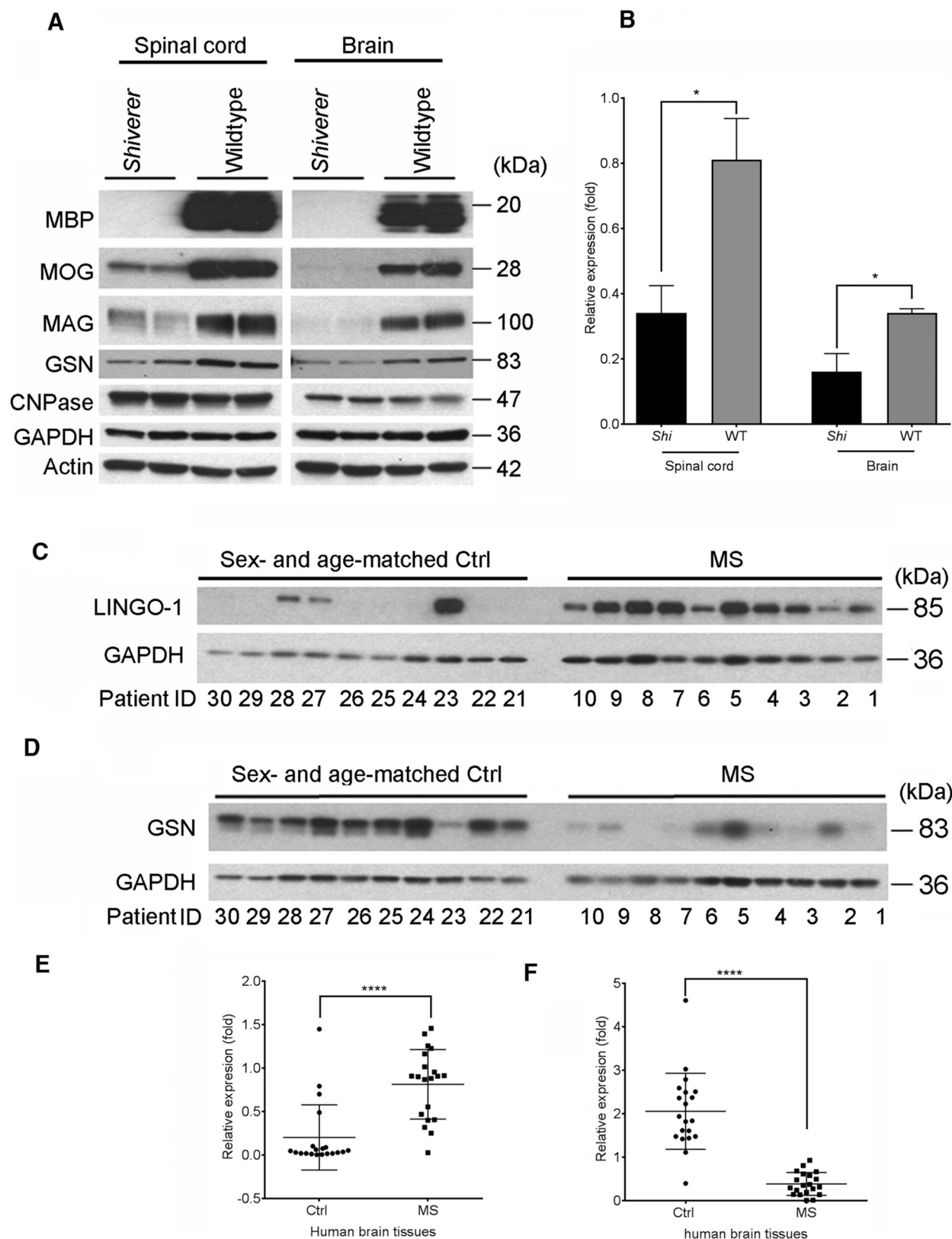


**Figure 4.** GSN is downregulated in *Shiverer* mice spinal cord and brain and human MS brain tissues. **A**, Western blot analysis of MBP, MAG, MOG, GSN, CNPase, GAPDH, and actin levels in spinal cord and brain lysates of P30 *Shiverer* mice or wild-type littermates. **B**, Quantification of the Western blot of GSN in **A**, represented as band intensity relative to GAPDH.  $p = 0.0491$  (spinal cord);  $p = 0.0487$  (brain); two-tailed unpaired Student's  $t$  test. **C**, Representative Western blot analysis of LINGO-1 from brain lysates of 10 human MS patients and 10 control samples (patient IDs correspond to the numbers listed in Table 1). **D**, Representative Western blot analysis of GSN from brain lysates of 10 human MS patients and 10 control samples (patient IDs correspond to the numbers listed in Table 1). **E**, Quantification of the Western blots for LINGO-1 from brain lysates of 20 human MS patients and 20 control samples using Image Studio software (LI-COR). Data are presented as band intensities relative to loading control (GAPDH).  $p < 0.0001$ ; two-tailed unpaired Student's  $t$  test. **F**, Quantification of the Western blots for GSN from brain lysates of 20 human MS patients and 20 control samples as done in **E**.  $p < 0.0001$ .



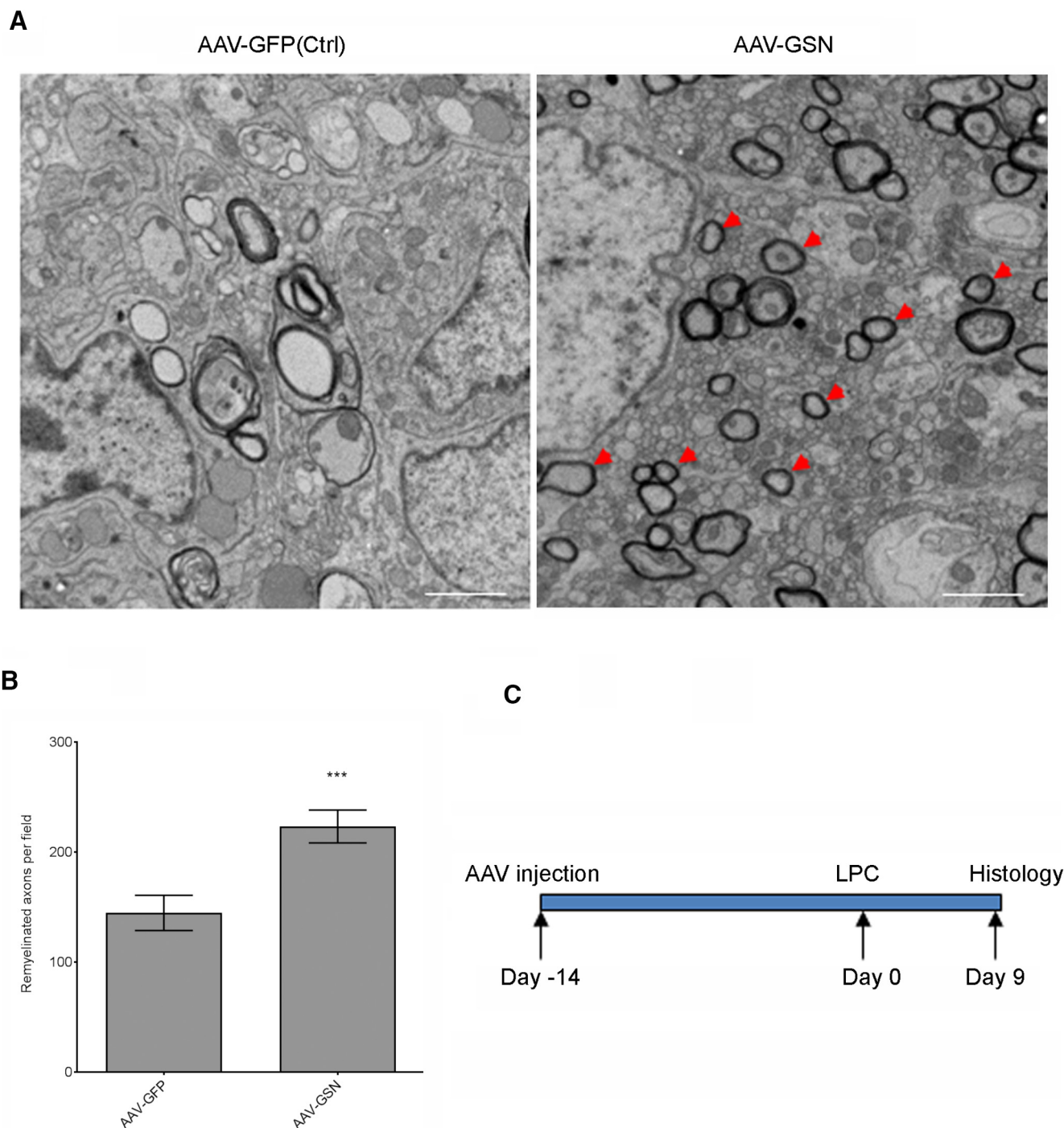


**Figure 5.** cGSN promotes remyelination in a rat LPC demyelination model. **A**, Remyelinated axons in the LPC-induced demyelination lesions were visualized by electron microscopy. Arrowhead denotes the remyelinated axon in a GSN-treated animal. Scale bar, 2  $\mu$ m. **B**, Quantification of remyelinated axons per field by toluidine blue staining from each treatment group.  $n = 30$  fields/3 animals/group.  $p = 0.0007$ ,  $t = 3.589$ , two-tailed unpaired Student's  $t$  test. **C**, Schematic diagram showing the experimental timeline.

sembly is required for OPC differentiation and, more importantly, suggest that cGSN, a key regulator of actin dynamics, plays a critical role for myelin sheet formation.

Gelsolin is a capping and severing actin-binding protein. pGSN functions to scavenge actin circulating in blood after tissue injury (Lee and Galbraith, 1992) and has been shown to decrease actin toxicity and inflammation in a murine model of MS (Li-ChunHsieh et al., 2015). The role of cGSN in regulating OPC intracellular actin for cell morphology is largely undefined. In this study, we demonstrated that cGSN plays an important

role for regulating OPC differentiation and maturation. cGSN overexpression facilitated OPC differentiation, whereas cGSN knockdown exerted an opposite effect. In *Shiverer* mice in which myelination was deficient due to lack of OPC terminal differentiation and maturation resulting from the lack of MBP protein (Seiwa et al., 2002), cGSN levels were also significantly reduced, along with other oligodendrocyte maturation markers (such as MOG and MAG). Conversely, the level of CNPase, which appears earlier than MBP (Reynolds and Wilkin, 1988; Pfeiffer et al., 1993), did not change. Therefore, increasing cGSN levels could

facilitate OPC differentiation and myelination, which could be critical for remyelination of demyelinated axons in the MS lesion. Decreased myelin thickness of optic nerves was observed in GSN knock-out mice (Zuchero et al., 2015). In general, the lack of severe phenotypes in knock-out mice due to compensatory effects appears to be a quite common phenomenon (Barbaric et al., 2007). Therefore, the lack of a severe phenotype on CNS myelination in GSN knock-out mice might be due to compensatory effects during development from other actin disassembly factors such as cofilin (Kronenberg et al., 2010; Nawaz et al., 2015). In our study, the dramatic inhibitory effect of cGSN siRNA on OPC differentiation *in vitro* may be due to the lack of the compensatory factors in an acute setting in 3 d cultures.

LINGO-1 is selectively expressed in the CNS in both oligodendrocytes and neurons (Mi et al., 2013). LINGO-1 functions by binding to a number of receptors on the cell surface, leading to activation or inactivation of downstream signaling pathways in a cell-type-dependent manner. For example, LINGO-1 forms complexes with NgR1 and p75 or Troy in neurons to activate RhoA pathway to inhibit neurite outgrowth (Mi et al., 2004; Park et al., 2005; Shao et al., 2005). LINGO-1 binds to EGFR in dopaminergic neurons and to TrkB in retinal ganglion cells, which blocks the respective EGF or BDNF pathways for neuronal survival (Inoue et al., 2007; Fu et al., 2010). In oligodendrocytes, LINGO-1 binds to ErbB2 to inhibit OPC terminal differentiation (Lee et al., 2014). Anti-LINGO-1 antibody treatment increased OPC differentiation, which was associated with increased production of MBP and other myelin-associated proteins. By studying this process, we discovered that blocking LINGO-1 promotes cGSN expression. Like anti-LINGO-1 antibody treatment, overexpression of cGSN increased OPC differentiation *in vitro* and remyelination *in vivo*. In contrast, overexpression of LINGO-1 or blocking cGSN by its siRNA blocked OPC differentiation. Coexpression of cGSN and LINGO-1 overcame the inhibitory effect of LINGO-1. Intriguingly, we observed that cGSN levels were significantly reduced in MS brains, in which OPC differentiation is stalled in the lesions (Chang et al., 2000) and LINGO-1 is highly expressed. Our findings suggest that cGSN works downstream of the LINGO-1 signaling pathway. How cGSN expression is regulated by LINGO-1 remains to be determined.

In summary, we discovered that LINGO-1 negatively regulates oligodendrocyte differentiation through the cGSN signaling pathway, thus identifying a novel role of cGSN in oligodendrocyte differentiation and maturation. This finding provides new insights into potential drug targets for CNS remyelination that can be used for the treatment of demyelination diseases such as MS.

## References

- Barbaric I, Miller G, Dear TN (2007) Appearances can be deceiving: phenotypes of knockout mice. *Brief Funct Genomic Proteomic* 6:91–103. [CrossRef Medline](#)
- Bauer NG, Richter-Landsberg C, Ffrench-Constant C (2009) Role of the oligodendroglial cytoskeleton in differentiation and myelination. *Glia* 57:1691–1705. [CrossRef Medline](#)
- Bercury KK, Macklin WB (2015) Dynamics and mechanisms of CNS myelination. *Dev Cell* 32:447–458. [CrossRef Medline](#)
- Bucki R, Levental I, Kulakowska A, Janney PA (2008) Plasma gelsolin: function, prognostic value, and potential therapeutic use. *Curr Protein Pept Sci* 9:541–551. [CrossRef Medline](#)
- Cadavid D, Klistorner A, Chai Y, Leocani L, Aktas O, Butzkueven H, Ziemssen T, Ziemssen F, Frederiksen J, Xu L; on behalf of the RENEW Investigators (2015) Evidence that the anti-LINGO-1 monoclonal antibody BIIB033 protects against multifocal visual evoked potential amplitude loss in the fellow eye of subjects with unilateral acute optic neuritis [Abstract]. Available from: <http://onlinelibrary.ectrims-congress.eu/ectrims/2015/31st/116697/diego.cadavid.evidence.that.the.anti-lingo-1.monoclonal.antibody.biib033.html?f=m3>. Accessed: October 7, 2015.
- Chang A, Nishiyama A, Peterson J, Prineas J, Trapp BD (2000) NG2-positive oligodendrocyte progenitor cells in adult human brain and multiple sclerosis lesions. *J Neurosci* 20:6404–6412. [Medline](#)
- Chernoff GF (1981) Shiverer: an autosomal recessive mutant mouse with myelin deficiency. *J Hered* 72:128. [Medline](#)
- dos Remedios CG, Chhabra D, Kekic M, Dedova IV, Tsubakihara M, Berry DA, Nosworthy NJ (2003) Actin binding proteins: regulation of cytoskeletal microfilaments. *Physiol Rev* 83:433–473. [CrossRef Medline](#)
- Fu QL, Hu B, Li X, Shao Z, Shi JB, Wu W, So KF, Mi S (2010) LINGO-1 negatively regulates TrkB phosphorylation after ocular hypertension. *Eur J Neurosci* 31:1091–1097. [CrossRef Medline](#)
- Inoue H, Lin L, Lee X, Shao Z, Mendes S, Snodgrass-Belt P, Sweigard H, Engber T, Pepinsky B, Yang L, Beal MF, Mi S, Isacson O (2007) Inhibition of the leucine-rich repeat protein LINGO-1 enhances survival, structure, and function of dopaminergic neurons in Parkinson's disease models. *Proc Natl Acad Sci U S A* 104:14430–14435. [CrossRef Medline](#)
- Kremer D, Küry P, Dutta R (2015) Promoting remyelination in multiple sclerosis: current drugs and future prospects. *Mult Scler* 21:541–549. [CrossRef Medline](#)
- Kremer IE, Evers SM, Jongen PJ, van der Weijden T, van de Kolk I, Hilgsmann M (2016) Identification and prioritization of important attributes of disease-modifying drugs in decision making among patients with multiple sclerosis: a nominal group technique and best-worst scaling. *PLoS One* 11:e0164862. [CrossRef Medline](#)
- Kronenberg G, et al. (2010) Impact of actin filament stabilization on adult hippocampal and olfactory bulb neurogenesis. *J Neurosci* 30:3419–3431. [CrossRef Medline](#)
- Kwiatkowski DJ, Stossel TP, Orkin SH, Mole JE, Colten HR, Yin HL (1986) Plasma and cytoplasmic gelsolins are encoded by a single gene and contain a duplicated actin-binding domain. *Nature* 323:455–458. [CrossRef Medline](#)
- Lee WM, Galbraith RM (1992) The extracellular actin-scavenger system and actin toxicity. *N Engl J Med* 326:1335–1341. [CrossRef Medline](#)
- Lee X, Shao Z, Sheng G, Pepinsky B, Mi S (2014) LINGO-1 regulates oligodendrocyte differentiation by inhibiting ErbB2 translocation and activation in lipid rafts. *Mol Cell Neurosci* 60:36–42. [CrossRef Medline](#)
- Li GH, Arora PD, Chen Y, McCulloch CA, Liu P (2012) Multifunctional roles of gelsolin in health and diseases. *Med Res Rev* 32:999–1025. [CrossRef Medline](#)
- Li-ChunHsieh K, Schob S, Zeller MW, Pulli B, Ali M, Wang C, Chiou TT, Tsang YM, Lee PS, Stossel TP, Chen JW (2015) Gelsolin decreases actin toxicity and inflammation in murine multiple sclerosis. *J Neuroimmunol* 287:36–42. [CrossRef Medline](#)
- Mei F, Mayoral SR, Nobuta H, Wang F, Despons C, Lorrain DS, Xiao L, Green AJ, Rowitch D, Whistler J, Chan JR (2016) Identification of the kappa-opioid receptor as a therapeutic target for oligodendrocyte remyelination. *J Neurosci* 36:7925–7935. [CrossRef Medline](#)
- Mi S, et al. (2009) Promotion of central nervous system remyelination by induced differentiation of oligodendrocyte precursor cells. *Ann Neurol* 65:304–315. [CrossRef Medline](#)
- Mi S, Lee X, Shao Z, Thill G, Ji B, Relton J, Levesque M, Allaire N, Perrin S, Sands B, Crowell T, Cate RL, McCoy JM, Pepinsky RB (2004) LINGO-1 is a component of the Nogo-66 receptor/p75 signaling complex. *Nat Neurosci* 7:221–228. [CrossRef Medline](#)
- Mi S, Miller RH, Lee X, Scott ML, Shulag-Morskaya S, Shao Z, Chang J, Thill G, Levesque M, Zhang M, Hession C, Sah D, Trapp B, He Z, Jung V, McCoy JM, Pepinsky RB (2005) LINGO-1 negatively regulates myelination by oligodendrocytes. *Nat Neurosci* 8:745–751. [CrossRef Medline](#)
- Mi S, Hu B, Hahm K, Luo Y, Kam Hui ES, Yuan Q, Wong WM, Wang L, Su H, Chu TH, Guo J, Zhang W, So KF, Pepinsky B, Shao Z, Graff C, Garber E, Jung V, Wu EX, Wu W (2007) LINGO-1 antagonist promotes spinal cord remyelination and axonal integrity in MOG-induced experimental autoimmune encephalomyelitis. *Nat Med* 13:1228–1233. [CrossRef Medline](#)
- Mi S, Pepinsky RB, Cadavid D (2013) Blocking LINGO-1 as a therapy to promote CNS repair: from concept to the clinic. *CNS Drugs* 27:493–503. [CrossRef Medline](#)
- Mikoshiba K, Aoki E, Tsukada Y (1980) 2'-3'-cyclic nucleotide 3'-phosphohydrolase activity in the central nervous system of a myelin deficient mutant (Shiverer). *Brain Res* 192:195–204. [CrossRef Medline](#)
- Najm FJ, et al. (2015) Drug-based modulation of endogenous stem cells promotes functional remyelination *in vivo*. *Nature* 522:216–220. [CrossRef Medline](#)

- Nawaz S, Sánchez P, Schmitt S, Snaidero N, Mitkovski M, Velte C, Brückner BR, Alexopoulos I, Czopka T, Jung SY, Rhee JS, Janshoff A, Witke W, Schaap IA, Lyons DA, Simons M (2015) Actin filament turnover drives leading edge growth during myelin sheath formation in the central nervous system. *Dev Cell* 34:139–151. [CrossRef Medline](#)
- Park JB, Yiu G, Kaneko S, Wang J, Chang J, He XL, Garcia KC, He Z (2005) A TNF receptor family member, TROY, is a coreceptor with Nogo receptor in mediating the inhibitory activity of myelin inhibitors. *Neuron* 45:345–351. [CrossRef Medline](#)
- Pfeiffer SE, Warrington AE, Bansal R (1993) The oligodendrocyte and its many cellular processes. *Trends Cell Biol* 3:191–197. [CrossRef Medline](#)
- Reynolds R, Wilkin GP (1988) Development of macroglial cells in rat cerebellum. II. An in situ immunohistochemical study of oligodendroglial lineage from precursor to mature myelinating cell. *Development* 102:409–425. [Medline](#)
- Ross PL, Huang YN, Marchese JN, Williamson B, Parker K, Hattan S, Khainovski N, Pillai S, Dey S, Daniels S, Purkayastha S, Juhasz P, Martin S, Bartlett-Jones M, He F, Jacobson A, Pappin DJ (2004) Multiplexed protein quantitation in *Saccharomyces cerevisiae* using amine-reactive isobaric tagging reagents. *Mol Cell Proteomics* 3:1154–1169. [CrossRef Medline](#)
- Seiwa C, Kojima-Aikawa K, Matsumoto I, Asou H (2002) CNS myelinogenesis in vitro: myelin basic protein deficient shiverer oligodendrocytes. *J Neurosci Res* 69:305–317. [CrossRef Medline](#)
- Shao Z, Browning JL, Lee X, Scott ML, Shulga-Morskaya S, Allaire N, Thill G, Levesque M, Sah D, McCoy JM, Murray B, Jung V, Pepinsky RB, Mi S (2005) TAJ/TROY, an orphan TNF receptor family member, binds Nogo-66 receptor 1 and regulates axonal regeneration. *Neuron* 45:353–359. [CrossRef Medline](#)
- Spinardi L, Witke W (2007) Gelsolin and diseases. *Subcell Biochem* 45:55–69. [CrossRef Medline](#)
- Thiruvalluvan A, Czepiel M, Kap YA, Mantingh-Otter I, Vainchtein I, Kuipers J, Bijlard M, Baron W, Giepmans B, Bruck W, Hart BA, Boddeke E, Copray S (2016) Survival and functionality of human induced pluripotent stem cell-derived oligodendrocytes in a nonhuman primate model for multiple sclerosis. *Stem Cell Transl Med* 5:1550–1561. [CrossRef Medline](#)
- Yao X, Su T, Verkman AS (2016) Clobetasol promotes remyelination in a mouse model of neuromyelitis optica. *Acta Neuropathol Commun* 4:42. [CrossRef Medline](#)
- Zuchero JB, Fu MM, Sloan SA, Ibrahim A, Olson A, Zaremba A, Dugas JC, Wienbar S, Caprariello AV, Kantor C, Leonoudakis D, Lariosa-Willingham K, Kronenberg G, Gertz K, Soderling SH, Miller RH, Barres BA (2015) CNS myelin wrapping is driven by actin disassembly. *Dev Cell* 34:152–167. [CrossRef Medline](#)